*Inorg. Chem.* **1997,** *36,* 339−344

# Properties of Fluorocarbonyl Peroxynitrate[†]

**Dieter Scheffler,[‡] Iris Schaper,[‡] Helge Willner,*[,‡] Hans-Georg Mack,[§] and Heinz Oberhammer*[,§]**

Institut für Anorganische Chemie der Universität Hannover, Callinstrasse 9,
D-30167 Hannover, Germany, and Institut für Physikalische und Theoretische Chemie der Universität
Tübingen, Auf der Morgenstelle 8, D-72076 Tübingen, Germany

*Received July 18, 1996*[⊗]

The synthesis of $FC(O)OONO_2$ is accomplished by the photolysis of a mixture of $(FCO)_2$, $NO_2$, and $O_2$. The pure product is isolated after trap-to-trap condensation and the removal of byproducts by treatment of the crude product with $O_3$ and $AsF_5$. The colorless liquid freezes at −105 °C; its boiling point is 32 °C. At 20 °C and a few millibars, $FC(O)OONO_2$ decomposes in the gas phase with a half-life of 20 h. $FC(O)OONO_2$ is characterized by vapor pressure measurements, vibrational, $^{19}F$ NMR, $^{13}C$ NMR and UV spectroscopies as well as by mass spectrometry. According to the vibrational and NMR spectra, the compound exists at room temperature only as a syn conformer. The molecular structure of $FC(O)OONO_2$ is determined by gas electron diffraction. The molecule possesses a skew structure with a dihedral angle of $\phi(COON) = 86.2(14)°$. The short O−O bond (1.420(6) Å) and the long N−O bond (1.514(6) Å) are consistent with the chemical properties of this compound. The experimental geometry is reproduced reasonably well by quantum chemical.

## Introduction

The atmospheric degradation of organic compounds is initiated by H-atom abstraction with OH or $NO_3$ radicals or Cl atoms. The organic radicals formed in this manner are rapidly converted by reaction with molecular oxygen into peroxy radicals. In the presence of $NO_2$, peroxynitrates are formed. Peroxyacetyl nitrate, $CH_3C(O)OONO_2$ (PAN), first identified by Stephens,[1] has been identified as one of the main constituents of photochemical smog at many places in the world.[2,3] Since this discovery, the kinetics, spectroscopic properties, and tropospheric chemistry of organic peroxy radicals and their temporary reservoirs, $RO_2NO_2$, have been investigated in detail.[4,5]

Hydrofluorocarbons (HFCs) and hydrochlorofluorocarbons (HCFCs) are considered as chlorofluorocarbons (CFC) replacements. These partially hydrogenated materials can in principle be degraded in the troposphere by reaction with OH, before they reach the stratosphere, to cause the loss of ozone. The environmental acceptability of these materials depends on the role that their photooxidation products play in the chemistry of the atmosphere. Therefore, the photochemistry of alternative halocarbons is being studied extensively.[6] In this context $FCO_x$ radicals are of special importance. For $FC(O)O_2$ radicals, the fluorocarbonyl peroxynitrate ($FC(O)OONO_2$) is a reservoir species. This interesting inorganic peroxide was first identified by IR spectroscopy,[7] and the kinetics of its formation, the thermal stability, and the implications for the atmospheric chemistry have been investigated recently.[8] However, pure $FC(O)OONO_2$ has so far not been isolated, and many of its properties are unknown. Because the FC(O) group is isoelectronic with $NO_2$, $FC(O)OONO_2$ can be viewed as the link between the stable peroxide $FC(O)OOC(O)F$,[9−11] known since 1960, and $O_2NOONO_2$. The latter is a postulated intermediate in the decomposition of $NO_3$ radicals into $NO_2$ and oxygen.[12,13]

## Experimental Section

*Caution!* Fluorocarbonyl peroxynitrate and ozone are potentially explosive, especially in the presence of organic materials. It is important to take appropriate safety precautions when these compounds are handled and to carry out reactions only in millimolar quantities.

**Materials and Apparatus.** Volatile materials were manipulated in a glass vacuum line equipped with a capacitance pressure gauge (221 AHS-1000 MKS Baratron, Burlington) and valves with PTFE stems (Young, London). The vacuum line was connected to an IR cell ($l = 200$ mm, Si windows 0.5 mm thick). It was hence possible to observe the purification process and to follow the course of reactions instantaneously. $FC(O)OONO_2$ was synthesized by the photolysis of a mixture of oxalyl fluoride ($(FCO)_2$), $NO_2$, and $O_2$. The photolysis device consisted of a 15 W low-pressure Hg lamp (TNN 15/32 Heraeus, Kleinostheim, Germany) surrounded by water-jacketed quartz tubes,

---

[†] Dedicated to Professor Dr. P. Sartori on the occasion of his 65th birthday.

[*] Authors to whom correspondence should be addressed.

[‡] Institut für Anorganische Chemie der Universität Hannover.

[§] Institut für Physikalische und Theoretische Chemie der Universität Tübingen.

[⊗] Abstract published in *Advance ACS Abstracts,* January 1, 1997.

(1) Stephens, E. R., Pitts, J. N., Metcalf, R. L., Eds. *Advances in Environmental Sciences*; Wiley-Interscience: New York, 1969; Vol. 1 pp 119−146.

(2) Darley, E. F.; Kettner, K. A.; Stephens, E. R. *Anal. Chem.* **1963**, *35*, 589.

(3) Nieboer, H.; van Ham, J. *Atmos. Environ.* **1976**, *10*, 115.

(4) Lightfoot, P. D.; Cox, R. A.; Crowley, J. N.; Destriau, M.; Hayman, G. D.; Jenkin, M. E.; Moortgat, G. K.; Zabel, F. *Atmos. Environ.* **1992**, *26A*, 1805.

(5) Wallington, T. J.; Dagaut, P.; Kurylo, M. J. *Chem. Rev.* **1992**, *92*, 667.

(6) Francisco, J. S.; Matti Marieq, M.; Neckers, D. C.; Volman, D. H.; von Bünau, G. *Advances in Photochemistry*; Wiley & Sons: New York, 1995; Vol. 20, pp 79−163.

(7) Edney, E. O., Spence, J. W., Hanst, P. L., Grosjean, D., Eds. *Peroxy Nitrate Air Pollutants: Synthesis and Thermal Stability, in Nitrogenous Air Pollutants*; Ann Arbor Science Publisher: Ann Arbor, MI, 1979; Chapter 6.

(8) Wallington, T. J.; Schneider, W. F.; Møgelberg, T. E.; Nielsen, O. J.; Sehested, J. *Int. J. Chem. Kinet.* **1995**, *27*, 391.

(9) Arvia, A. J.; Aymonino, P. J.; Waldow, C. H.; Schumacher, H. J. *Angew. Chem.* **1960**, *72*, 169.

(10) Della Védova, C. O.; Mack, H. G. *J. Mol. Struct.* **1992**, *274*, 25.

(11) Mack, H. G.; Della Védova, C. O.; Oberhammer, H. *Angew. Chem.* **1991**, *103*, 1166.

(12) Khadzhi-Ogly, M. R.; Yagodovskaya, T. V.; Nekrasov, L. I. *Z. Fiz. Khim.* **1981**, *55*, 3124.

(13) Matthews, R. W.; Mahlman H. A.; Sworski, T. J. *J. Phys. Chem.* **1972**, *19*, 2686.

which were placed in the middle of a 5 L glass round-bottom flask. The outside of the flask was cooled to 2 °C via a Kryomat (Lauda RC6) and connected to the vacuum line via a flexible stainless steel bellow tube. After evacuation of the device, the inner surface was conditioned with $N_2O_5$ vapor (10−20 mbar) for a couple hours, to remove residual water from the surface. Subsequently, the bulb was charged to a pressure of 40 mbar with $(FCO)_2$ (9 mmol), to a total pressure of 100 mbar with $NO_2$ (13 mmol) and to 900 mbar with $O_2$ (160 mmol). The course of the photochemical reaction was followed by removing small samples every 3−5 h for infrared analysis. The reaction was stopped after the bands of $(FCO)_2$ had disappeared (after ~30 h). The content of the bulb was slowly pumped through three U-traps kept at −196 °C to remove oxygen from the reaction mixture. Then the most volatile side products ($CO_2$, $COF_2$) were pumped off at −80 °C, identified by IR, and discarded in small batches until the first bands of $FC(O)OONO_2$ appeared. Subsequently the residue was transferred into a 200 mL round-bottom flask at −196 °C. With slow warming, the most volatile products were collected at −196 °C in a U-trap, until all $FC(O)OONO_2$ had evaporated. The residue in the round flask ($N_2O_4$) was discarded. The above procedure was repeated until the $FC(O)OONO_2$ content had reached ~60%. Further purification by fractional condensation or evaporation was not possible. Finally, the impurities $NO_2$ and $CH_3C(O)F$ (impurity found in the starting material $(FCO)_2$) were removed by treatment with either $O_3$ or $AsF_5$. Batches (2 mmol) of the crude product together with 1.5 mmol of $O_3$ were trapped in a 200 mL round bottom flask kept at −196 °C. After the contents had slowly warmed to room temperature, the $O_2$ formed was pumped off at −196 °C and the residue was fractionated through a series of traps held at −196, −128, and −90 °C. $FC(O)OONO_2$ (free of $NO_2$) was collected in the trap held at −128 °C. The byproduct $CH_3C(O)F$ was removed with a small excess of $AsF_5$ at −60 °C in a manner similar to that described above. No impurities were detectable by IR and $^{19}F$ NMR spectroscopy in the final product (2 mmol).

Oxalyl fluoride was synthesized by the reaction of oxalyl chloride (>98% Merck) with triethylamine trihydrofluoride (Hoechst) in $CH_3CN$ solution.[14] Oxygen (99.999%, Linde) and $NO_2$ (Union Carbide) were obtained from commercial sources and used without further purification. Ozone was made in an ozonizer (Model 301, Sander, Eltze, Germany) and trapped using liquid oxygen to prevent condensation of oxygen. Oxygen, dissolved in ozone was removed in vacuo at −196 °C. NO was synthesized by reduction of dilute $HNO_3$ with Cu powder. $AsF_5$ was prepared by burning As in an excess of fluorine. Both compounds were purified by trap-to-trap distillation in vacuo. $(FCO)_2$, $O_3$, NO, $AsF_5$, and $FC(O)OONO_2$ were stored in flame-sealed glass ampules in liquid nitrogen. The ampules were opened and resealed by use of an ampule key, which was described previously.[15]

**Instrumentation. (a) Vibrational Spectroscopy.** Gas phase infrared spectra in the range 4000−400 $cm^{-1}$ were recorded with a resolution of 2 $cm^{-1}$ using an FTIR instrument (Nicolet Impact 400 D) which was directly coupled with the vacuum line. Matrix infrared spectra were recorded with a resolution of 1.2 $cm^{-1}$ using the Bruker IFS66v FTIR spectrometer. A DTGS detector together with a Ge/KBr beam splitter operated in the region 4000−400 $cm^{-1}$, and 64 scans were coadded for each spectrum. A DTGS detector together with a 6 $\mu$m Mylar beam splitter was used in the region 550−80 $cm^{-1}$; 128 scans were coadded for each spectrum with a resolution of 2 $cm^{-1}$. Details of the matrix isolation apparatus are given elsewhere.[16]

FT-Raman spectra of liquid $FC(O)OONO_2$ were recorded with the Bruker FRA-106 FT Raman accessory mounted on the optical bench of the IFS66v instrument using the 1064 nm exciting line of a Nd-YAG laser (Adlas, DPY 301, Lübeck, Germany).

**(b) NMR Spectroscopy.** The $^{19}F$ and $^{13}C$ NMR spectra of pure liquid samples were recorded with a Bruker MSL 200 spectrometer and a $^{19}F/^{1}H$ dual or for $^{13}C$ a multinuclear probe head, operating at 188.31 and 50.33 MHz, respectively. A 5 mm diameter tube containing the neat $FC(O)OONO_2$ sample was centered inside a 10 mm tube containing the lock $CD_3OD$ and the reference $CFCl_3$.

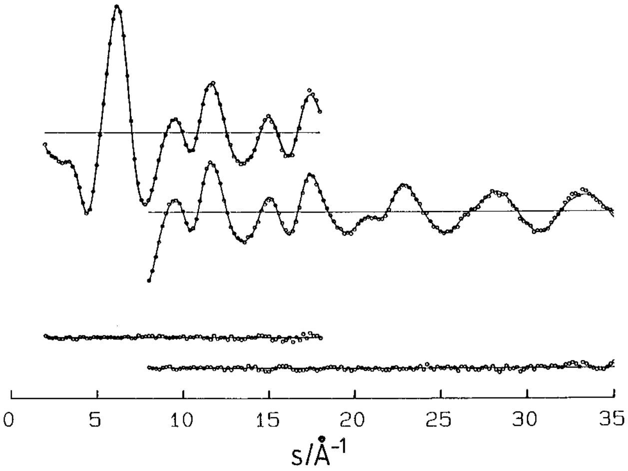

**Figure 1.** Experimental (dots) and calculated (full line) molecular intensities for long (above) and short (below) nozzle-to-plate distances and differences.

**(c) Mass Spectrometry.** Mass spectra were recorded with a MAT 112-S mass spectrometer with a resolution of 1:800 and an ionization energy of 70 eV. The gas flow into the ion source from a sample reservoir held at −60 °C was achieved via a glass tube attached to a PTFE needle valve (Young).

**(d) UV Spectroscopy.** UV spectra were recorded with a 1024 diode array spectrometer (Spectroscopy International). As a light source a CLD 30 W deuterium lamp (Hamamatsu) was employed. Hg emission lines from pen lamps (Oriel) were used for wavelength calibrations. Gas phase spectra were recorded in a Duran (Schott) glass cell (optical path length, 10 cm) equipped with quartz windows (Suprasil, Heraeus). Pressures were measured with a capacitance manometer (MKS Baratron 122 A, 100 mbar absolute). To eliminate absorption from atmospheric $O_2$, the monochromator and the housing of the absorption cell were flushed with $N_2$.

**(e) Melting Point and Vapor Pressure.** The melting point was determined with a sample placed inside a 6 mm glass tube, using a stirred isopentane cold bath in a transparent Dewar glass vessel. The temperature was measured with a small (5 × 1 mm) Pt 100 resistance sensor (Heraeus), attached to the sample tube. Vapor pressures were measured with a capacitance manometer (MKS Baratron 122 A, 1000 mbar absolute) in the temperature range between +14 and −50 °C.

**(f) Electron Diffraction.** The electron diffraction intensities were recorded with a Balzers KD-G2[17] gas diffractograph at two nozzle-to-plate distances (25 and 50 cm) with an accelerating voltage of ~60 kV. The electron wavelength was determined from ZnO diffraction patterns. A sample reservoir filled with 200 mg of pure $FC(O)OONO_2$ was cooled to ~−50 °C. The inlet system and the nozzle were kept at room temperature. The photographic plates were analyzed by the usual procedure.[18] The averaged molecular intensities in the *s*-ranges of 2−18 and 8−35 $Å^{-1}$ are presented in Figure 1.

## Results and Discussion

**Synthesis and Thermal Properties of $FC(O)OONO_2$.** The synthesis of pure $FC(O)OONO_2$ in 500 mg quantities by the photolysis of a mixture of $(FCO)_2$, $NO_2$, and $O_2$ is difficult and time consuming. This is due to the low yield of the desired product and the complicated purification procedure. The initial step in the synthesis is the 254 nm photolysis (low-pressure Hg lamp) of oxalyl fluoride, which yields FCO radicals,[19]

---

(14) Franz, R. *J. Fluorine Chem.* **1980**, *15*, 423.

(15) Gombler, W.; Willner, H. *J. Phys. E: Sci. Instrum.* **1987**, *20*, 1286.

(16) Argüello, G. A.; Grothe, H.; Kronberg, M.; Mack, H. G.; Willner, H. *J. Phys. Chem.* **1995**, *99*, 17525.

(17) Oberhammer, H. *Molecular Structure by Diffraction Methods*; Chemical Society: London, 1976; Vol. 4, p 24.

(18) Oberhammer, H.; Gombler, W.; Willner, H. *J. Mol. Struct.* **1981**, *70*, 273.

(19) Ahonkhai, S. I.; Nölle, A.; Behr, P.; Heydtmann, H. *J. Photochem. Photobiol. A: Chem.* **1994**, *80*, 389.

$$(FCO)_2 + h\nu \xrightarrow{254\ \mathrm{nm}} 2FCO \tag{1}$$

$$(FCO)_2 + h\nu \xrightarrow{254\ \mathrm{nm}} COF_2 + CO \tag{2}$$

but may also release $COF_2$ and CO. The branching ratio into the channels 1 and 2 is unknown, and theoretical calculations favor channel 2.[20] The absorption cross sections at 254 nm of the starting materials $(FCO)_2$ and $NO_2$ and of the product $FC(O)OONO_2$ are all in the same order of magnitude ($10^{-19}$ cm$^2$), and therefore the product can also undergo photodecomposition.

Fast reactions of FCO with $O_2$ and finally with $NO_2$ lead to the product:

$$FCO + O_2 + M \rightarrow FC(O)O_2 + M \tag{3}$$

$$FC(O)O_2 + NO_2 + M \rightarrow FC(O)OONO_2 + M \tag{4}$$

The yield of $FC(O)OONO_2$ is limited by the formation of FCO radicals, by hydrolysis of $FC(O)OONO_2$ on the glass walls of the reactor, and by its photolysis during the synthesis. Further possible side reactions of FCO radicals are

$$FCO + NO_2 + M \rightarrow FC(O)NO_2 + M \tag{5}$$

or

$$FCO + NO_2 + M \rightarrow FC(O)ONO + M \tag{6}$$

but neither $FC(O)NO_2$ nor FC(O)ONO (both are unknown) is observed by IR spectroscopy during synthesis. $FC(O)NO_2$ or FC(O)ONO may in principle decay rapidly

$$FC(O)NO_2 \rightarrow CO_2 + FNO \tag{7}$$

All these side and decomposition reactions during the synthesis of $FC(O)OONO_2$ are responsible for the low overall yield of ~10%.

Traces of a new product that is less volatile than $FC(O)OONO_2$ and has its strongest IR bands at 1910, 1763, 1302, and 1194 cm$^{-1}$ were detected during the purification process. These properties indicate formation of a fluorocarbonyl nitrate with a longer oxygen chain according to

$$FC(O)O_2 + NO_3 + M \rightarrow FC(O)OOONO_2 + M \tag{8}$$

Pure $FC(O)OONO_2$ is a colorless liquid with a freezing point of −105 °C. As expected, FC(O)OOC(O)F, the isoelectronic species of higher symmetry, possesses a higher freezing point of −43 °C. The boiling point extrapolated from the vapor pressure curve, $\log p = -1556/T + 8.108$ ($p$ in mbar, $T$ in K) recorded between −50 and +14 °C is 32 °C. The boiling point of FC(O)OOC(O)F (16 °C)[9] is lower, as expected, because FC(O) compounds are generally more volatile than $NO_2$ compounds. The respective boiling point pairs, 1.5 ($(FCO)_2$)[14] versus 21 °C ($N_2O_4$),[21] −47 (FC(O)Cl)[21] versus −14 °C ($NO_2Cl$),[21] and −59 (FC(O)OF)[22] versus −45 °C ($NO_2OF$),[21] serve as illustration.

The thermal decomposition of gaseous $FC(O)OONO_2$ in a glass cell was followed by IR spectroscopy. Initially the decay of the band at 1194 cm$^{-1}$ of a sample at 2 mbar and at 31 °C was found to be first order, with a rate constant $k$ of about 5 × $10^{-5}$ s$^{-1}$. After 2 h, $k$ was ~1 × $10^{-5}$ s, and after ~20 h, half of the sample had decomposed. $CO_2$, $HNO_3$, $NO_2$, and $SiF_4$ were identified as decomposition products. The primary step in this decomposition is

$$FC(O)OONO_2 + M \rightarrow FC(O)OO + NO_2 + M \tag{9}$$

With increasing $NO_2$ concentration the reaction rate decreases.

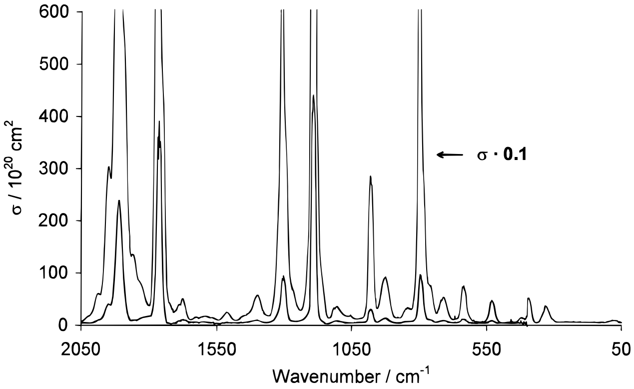

**Figure 2.** IR spectra of $FC(O)OONO_2$ in the gas phase.

In order to measure the reaction rate $k_9$, pure samples of $FC(O)OONO_2$ (2 mbar) were mixed with 100 or 400 mbar of NO, respectively. The decay of the band at 1194 cm$^{-1}$ followed during several hours first-order kinetics with $k_{obs} = 3.28 \times 10^{-4}$ and $4.68 \times 10^{-4}$ s$^{-1}$, respectively. These results are in good agreement with the data of Wallington et al.[8] The reaction products $CO_2$, $NO_2$, and $SiF_4$ are observed in a molar ratio of 1:0.6:0.2.

**Spectroscopic Properties. (a) Vibrational Spectra.** Figure 2 shows the gas phase infrared spectrum of $FC(O)OONO_2$. Vibrational data observed in the gas phase, in a neon matrix, and for a liquid sample together with tentative assignments and a comparison with data for FC(O)OOC(O)F are listed in Table 1. The uncertainties of the absorption cross sections are estimated to be ±5%.

As in most other peroxides, the substituents FCO and $NO_2$ have a gauche orientation relative to each other. The FC(O)OO and $O_2NOO$ moieties are expected to be planar or nearly planar. Two rotamers are possible with the $FC(O)O_2$ moiety oriented

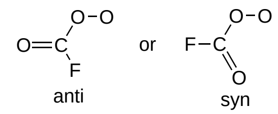

(10)

In order to observe and assign the individual vibrational spectra of these isomers, thermal effusive molecular beams of equilibrium mixtures between room temperature and 400 °C were trapped in neon matrices. The principal differences in the vibrational spectra of the isomers are expected in the C=O (1900 cm$^{-1}$) and C−F (1200 cm$^{-1}$) stretching region, but no additional bands were present, and between 20 and 250 °C, no changes in band intensites were observed. At higher temperatures, the compound decomposed into $NO_2$ and FC(O)OO radicals. Therefore it is most likely that only one isomer exists in this temperature range, but an assignment to either the anti or syn form is not possible based solely on the vibrational spectrum.

Due to the low symmetry ($C_1$) of $FC(O)OONO_2$, all 18 fundamentals are infrared and Raman active. These 18 fundamentals can be separated into 7 stretching, 8 deformation, and 3 torsional modes. In the high-wavenumber range all stretching

---

(20) Zhao, Y.; Francisco, J. S. *Chem. Phys. Lett.* **1992**, *199*, 65.
(21) Brauer, G., Ed. *Handbuch der Präparativen Anorganischen Chemie*; Enke: Stuttgart, Germany 1974; Vol. 1.
(22) Argüello, G. A.; Balzer-Jöllenbeck, G.; Jülicher, B.; Willner, H. *Inorg. Chem.* **1995**, *34*, 603.

**Table 1.** Vibrational Wavenumbers ($cm^{-1}$) for $FC(O)O_2NO_2$ and Their Assignments in Comparison to $[FC(O)O]_2$

| IR (gas) | $\sigma^a$ | Ne matrix | $I^b$ | Raman (liquid) | ab initio$^c$ | assignment/description of mode | | $[FC(O)O]_2{}^d$ | description of mode |
|---|---|---|---|---|---|---|---|---|---|
| R 3509 | 1.92 | | | | | | | | |
| Q 3503 | | 3503.0 | 0.5 | | | $2\nu_2$ | | | |
| R 3053 | 15.0 | | | | | | | | |
| Q 3048 | | 3047.2 | 2 | | | $\nu_2 + \nu_3$ | | | |
| R 2600 | 2.42 | | | | | | | | |
| Q 2596 | | 2594.7 | 0.5 | | | $2\nu_3$ | | | |
| 2375 | 5.04 | 2373.7 | 1 | | | $2\nu_4$ | | | |
| 2162 | 3.43 | 2166.7 | 0.5 | | | $\nu_4 + \nu_5$ | | | |
| | | 1960.1 | 3 | | | $2\nu_5$ | | | |
| 1948 | 30.3 | 1917.0 | 28 | | | $\nu_5 + \nu_6$ | | | |
| 1910 | 235 | 1902.5 | 26 | 1890 m | 1933 | $\nu_1$ | $\nu(C{=}O)$ | 1929 | $\nu_{as}$ (C=O) |
| R 1768 | 356 | | | | | | | | |
| Q 1763 | | 1762.6 | 43 | 1753 w | 1722 | $\nu_2$ | $\nu_{as}(NO_2)$ | 1902 | $\nu_s$ (C=O) |
| 1399 | 5.35 | 1378.1 | 1 | 1395 w | | $\nu_5 + \nu_{12}$ | | | |
| R 1307 | 87.3 | | | | | | | | |
| Q 1302 | | 1302.0 | 15 | 1298 s | 1430 | $\nu_3$ | $\nu_s$ ($NO_2$) | 1220 | $\nu_s$ (CF) |
| 1194 | 437 | 1191.7 | 100 | | 1265 | $\nu_4$ | $\nu$ (CF) | 1178 | $\nu_{as}$ (CF) |
| 981 | 28.5 | 983.3 | 8 | 978 w | 1123 | $\nu_5$ | $\nu$ (C−O) | 1018 | $\nu_s$ (C−O) |
| 925 | 8.94 | 926.0 | 5 | 928 s | 913 | $\nu_6$ | $\nu$ (O−O) | 914 | $\nu$ (O−O) |
| 795 | 95.2 | 792.0 | 32 | 787 m | 846 | $\nu_7$ | $\delta$ ($NO_2$) | 935 | $\nu_{as}$ (C−O) |
| 712 | 4.88 | 756.5 | 2 | 731 w | 737 | $\nu_8$ | $\delta$ oop COF | 751 | $\delta$ oop COF |
| | | 703.2 | 2 | | | | | | |
| R 640 | 6.95 | | | | | | | | |
| Q 635 | | 631.3 | 3 | 633 m | 709 | $\nu_9$ | $\delta$ oop $NO_2$ | 681 | |
| 530 | 4.38 | 530.0 | 3 | 529 m−s | 672 | $\nu_{10}$ | $\delta$ (COF) | 661 | $\delta$ (COF) |
| ~475 | | | | 461 m | 654 | $\nu_{11}$ | $\nu$ (O−$NO_2$) | 586 | |
| 420 | 2 | | | 421 sh | 580 | $\nu_{12}$ | $\rho$ (COF) | 480$^e$ | $\rho$ (COF) |
| 395 | 5 | | | 394 s | 402 | $\nu_{13}$ | $\rho$ ($NO_2$) | | |
| 343 | 2 sh | | | | 352 | $\nu_{14}$ | $\delta$ (OO−COF) | 406 | $\delta$ (OO−COF) |
| 331 | 2 | | | 324 s | 310 | $\nu_{15}$ | $\delta$ (OO−$NO_2$) | 345$^e$ | $\delta$ (OO−COF) |
| | | | | 220 m−w | 112 | $\nu_{16}$ | $\tau$ (O−O) | | |
| ~75 | <1 | | | | 85 | $\nu_{17}$ | $\tau$ (−COF) | 95$^e$ | $\tau$ (−COF) |
| | | | | | 72 | $\nu_{18}$ | $\tau$ ($NO_2$) | | |

[a] Absorption cross section in $10^{-20}$ $cm^2$. [b] Relative integrated Intensities $I(\nu_4) \equiv 100$. [c] Scaled HF/3-21G values; see text. [d] Reference 10. [e] IR(gas), this work.

**Table 2.** Absorption Cross Sections of Gaseous $FC(O)O_2NO_2$ at 25 °C

| $\lambda$/nm | $10^{20}\sigma/cm^2$ | $\lambda$/nm | $10^{20}\sigma/cm^2$ |
|---|---|---|---|
| 190 | 378 | 245 | 16.8 |
| 195 | 292 | 250 | 13.1 |
| 200 | 221 | 255 | 10.0 |
| 205 | 154 | 260 | 7.4 |
| 210 | 101 | 265 | 5.3 |
| 215 | 68.2 | 270 | 3.7 |
| 220 | 52.1 | 275 | 2.5 |
| 225 | 41.2 | 280 | 1.7 |
| 230 | 33.4 | 285 | 1.2 |
| 235 | 26.9 | 290 | 0.8 |
| 240 | 21.4 | | |

modes are easy assignable, except $\nu(O{-}NO_2)$, which is expected below 500 $cm^{-1}$. In the low-wavenumber range, where the torsional modes also appear, the bending modes are assigned by comparison to the reported, corresponding modes of FC(O)OOC(O)F,[10] FC(O)OF,[23] and $O_2NOF$.[24]

The $NO_2$ stretching modes at 1763 and 1302 $cm^{-1}$ can be used to ascertain the presence of the $O_2NOOX$ moiety within $FC(O)OONO_2$. According to Siebert,[25] $\nu_{av} = [(\nu_{as}{}^2 + \nu_s{}^2)/2]^{0.5}$ of the $NO_2$ stretching vibrations in $O_2NOX$ molecules increases with increasing electronegativity of X. The value of $\nu_{av}$ for $FC(O)OONO_2$ (1550 $cm^{-1}$) fits well to $FONO_2$ ($\nu_{av} = 1548$ $cm^{-1}$) and $ClONO_2$ ($\nu_{av} = 1533$ $cm^{-1}$).

**(b) $^{19}F$ and $^{13}C$ NMR Spectra.** As mentioned, the FC(O) group in $FC(O)OONO_2$ can be oriented syn or anti with respect to the O−O bond (eq 10). As observed previously in the case of FC(O)OF [22] (−38.3 and −21.2 ppm for F−C trans and cis to O−F, respectively), both rotamers are expected to resonate at different frequencies in the $^{19}F$ NMR spectrum. Only one signal, however, is observed in the range +20 to −90 °C. The signal shifts from −32.3 ppm at 20 °C to −31.0 ppm at −90 °C and broadens to 30 Hz at −30 °C. This behavior is explained by the motion of the $NO_2$ group. On the NMR time scale, free rotation occurs at room temperature but is frozen out at −90 °C and coalescence occurs at −30 °C. The chemical shift of −32 ppm and the $^{13}C-^{19}F$ coupling constant of 307 Hz fit very well to the series of syn FC(O)OX compounds, where X is F (−38.3 ppm, 300 Hz),[22] OC(O)F (−37.9 ppm, 302 Hz),[22] or OF (−31.3 ppm, 312 Hz).[22] Because the respective NMR data for anti FC(O)OF (−21.2 ppm, 330 Hz)[22] are significant different, it is concluded that $FC(O)OONO_2$ exists as the syn rotamer only.

The $^{13}C$ chemical shift of $FC(O)OONO_2$ is observed at 144.8 ppm relative to TMS.

**(c) UV Spectrum.** In the UV region, gaseous $FC(O)OONO_2$ shows an unstructured absorption ranging from 290 nm with increasing intensity to 190 nm. The absorption cross sections were obtained from four spectra at pressures of the sample between 1 and 30 mbar which are listed in Table 2. The uncertainties of the absorption cross sections are estimated to be ±5%. The UV spectrum is very similar in shape to the spectrum of FC(O)OOC(O)F[22] but more intense by a factor of ~10. The absorption may be assigned to a n → $\pi^*$ transition of the FC(O) and $NO_2$ chromophors.

---

(23) Argüello, G. A.; Jülicher, B.; Ulic, S. E.; Willner, H.; Casper, B.; Mack, H. G.; Oberhammer, H. *Inorg. Chem.* **1995**, *34*, 2089.

(24) Casper, B.; Dixon, A. D.; Mack, H. G.; Ulic, S. E.; Willner, H.; Oberhammer, H. *J. Am. Chem. Soc.* **1994**, *116*, 8317.

(25) Siebert, H. *Anwendungen der Schwingungsspektroskopie in der Anorganischen Chemie*; Springer Verlag: Berlin, 1966; p 96.

**Table 3.** Experimental and calculated geometric parameters for $FC(O)OONO_2$

| | GED[a] | | HF/3-21G | LDF/DZP[b] |
|---|---|---|---|---|
| O−O | 1.420 (6) | $p_1$ | 1.436 | 1.390 |
| O−C | 1.355 [10][c] | | 1.380 | 1.371 |
| O−N | 1.514 (6) | $p_2$ | 1.492 | 1.524 |
| C═O | 1.165 [10][c] | | 1.171 | 1.189 |
| C−F | 1.320 [10][c] | | 1.321 | 1.320 |
| N═O4 | 1.192 (4) | $p_3$ | 1.204 | 1.198 |
| N═O5 | 1.192 (4) | $p_3$ | 1.209 | 1.199 |
| O2−O1−C | 107.5 (10) | $p_4$ | 109.8 | 109.0 |
| O1−O2−N | 106.7 (12) | $p_5$ | 107.0 | 109.4 |
| O1−C═O3 | 128.8 [10][c] | | 128.1 | 128.2 |
| O1−C−F | 104.3 [10][c] | | 105.3 | 104.6 |
| $(O2-N{=}O)_{mean}$ | 114.4 (6) | $p_6$ | 113.3 | 112.6 |
| (O2−N═O5) − (O2−N═O4) | 7.0 [10][d] | | 5.9 | 7.8 |
| O2−N═O4 | 110.9 (8) | | 110.3 | 108.7 |
| O2−N═O5 | 117.9 (8) | | 115.2 | 116.5 |
| $\tau$ (FCO)[e] | 5.6 (43) | $p_7$ | 1.2 | 6.9 |
| $\tau$ ($NO_2$)[e] | 4.9 (9) | $p_8$ | 11.6 | 0.1 |
| $\phi$ (C−O−O−N) | 86.2 (14) | $p_9$ | 86.2 | 79.4 |

[a] $r_a$ distances (Å) and $\angle_\alpha$ angles (deg). Experimental uncertainties in parentheses are $3\sigma$ values and include systematic errors due to constraints (see text). For atom numbering, see Figure 3. [b] Results from ref 8. [c] Value constrained to that in $(C(O)F)_2O_2$ with estimated uncertainty in brackets. [d] Value constrained to theoretical result with estimated uncertainty in brackets. [e] Torsion of the FC(O) and $NO_2$ groups around O−C and O−N bonds, respectively. For $\tau = 0°$ the C═O3 and N═O5 bonds exactly eclipse the O−O bond. Both torsions lead to a decrease of the O3···O5 distance.

**(d) Mass Spectrum.** The 70 eV mass spectrum of $FC(O)OONO_2$ shows the following fragment ion pattern, *m/z* (%, ion): 63 (6, $FCO_2^+$), 62 (3, $NO_3^+$), 47 (51, $FCO^+$), 46 (100, $NO_2^+$), 44 (48, $CO_2^+$), 32 (23, $O_2^+$), 30 (35, $NO^+$), 28 (46, $CO^+$). The appearance of the base peak $NO_2^+$, is in accordance with the high stability of this cation and the weak $O-NO_2$ bond. The weak $O-NO_2$ bond appears also to be responsible for our inability to detect a parent ion peak. Further fragmentation is similar to that observed for FC(O)OOC(O)F.[22]

**Theoretical Calculations.** Earlier theoretical calculations in combination with experimental studies for FC(O)OOC(O)F[11] and $XONO_2$ with X = F[24] or Cl[26] demonstrated that geometric structures for such compounds are reproduced considerably better with the low-level ab initio method HF/3-21G than with higher level calculations such as HF/6-31G* or MP2/6-31G*. Also, the local density functional theory method (LDF/TZP) reproduces the N−O single bond distance in $FONO_2$ correctly. LDF calculations (VWN local exchange−correlation potential and DZP basis set) for the syn conformer of $FC(O)OONO_2$ have been reported by Wallington et al.[8] Since we were interested primarily in approximate vibrational amplitudes for the electron diffraction analysis, we performed additional ab initio calculations for the syn form with the HF/3-21G method.[27] It is well-known that vibrational amplitudes do not depend strongly on the force field, and therefore, a low-level method is sufficient for this purpose. The optimized geometric parameters are included in Table 3. Internal force constants were derived from the calculated Cartesian force constants and scaled with the usual factor 0.85, except for the N═O stretching constants and the three constants for torsion around the O−O, O−C and O−N single bonds. Whereas the HF/3-21G method overestimates in general vibrational frequencies, the N═O vibrations for the nitrates and for $FC(O)OONO_2$ are strongly underestimated. With a scaling factor of 1.40 for the N═O force constants, the calculated frequencies approximately reproduce the experimental values (see Table 1). Little experience exists about the reliability of calculated torsional force constants, and their scaling factors were set to 1.0. The vibrational amplitudes, which were calculated with the program ASYM40,[28] agree rather well with the refined experimental values (Table 4). Furthermore, the geometry of the anti conformer of $FC(O)OONO_2$ has been optimized and its energy is predicted to be 1.8 kcal mol$^{-1}$ higher than that of the syn form.

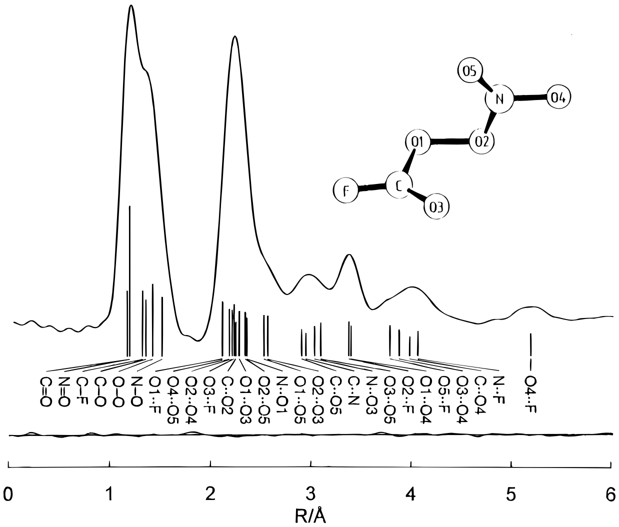

**Figure 3.** Experimental radial distribution function. The positions of interatomic distances are indicated by vertical bars.

## Gas Phase Structure

The radial distribution function (RDF) was derived by Fourier transform of the molecular electron diffraction intensities. An artificial damping function $\exp(-\gamma s^2)$ with $\gamma = 0.0019$ Å$^2$ was applied. The range of the RDF (Figure 3) for $r > 2.5$ Å can be reproduced only with a syn conformer. Planar FC(O) and $NO_2$ groups were assumed in the analysis. This assumption is in accord with ab initio calculations which predict deviations from planarity of these groups to be less than 1°. Preliminary geometric parameters derived from the RDF were refined by least-squares fitting of the molecular intensities. The intensities were modified with a diagonal weight matrix, and known complex scattering factors were used.[29] Figure 3 demonstrates that in this compound bonded distances and 1,3-nonbonded distances are very closely spaced. This causes large correlations between bonded distances and between bond angles. In order to reduce these correlations, the geometric parameters of the FC(O) group, i.e., C═O, C−F, O−C, O1−C═O3 and O1−C−F were constrained to those derived for FC(O)OOC(O)F.[11] Furthermore, the two N═O bond lengths were assumed to be equal and a mean value for the O2−N═O angles, $(O2-N{=}O)_{mean}$, was refined. The difference (O2−N═O5) − (O2−N═O4) was set to the theoretically calculated value. For all constrained geometric parameters, uncertainties of ±0.01 Å and ±1.0° were estimated. Corresponding systematic errors due to these constraints are included in the error limits for all refined parameters, in addition to $3\sigma$ values. In the least-squares refinement, the FC(O)OO and $O_2NOO$ moieties were allowed

---

(26) Casper, B.; Lambotte, P.; Minkwitz, R.; Oberhammer, H. *J. Phys. Chem.* **1993,** *97*, 9992.

(27) Frisch, M. J.; Trucks, G. W.; Schlegel, H. B.; Gill, W.; Johnson, B. G.; Wong, M. W.; Foresman, J. B.; Robb, M. A.; Head-Gordon. M.; Replogle, E. S.; Gomperts, R.; Andres, J. L.; Raghavachari, K.; Binkley, J. S.; Gonzales, C.; Martin, R. L.; Fox, D. J.; Defrees, D. J.; Baker, J.; Stewart, J. J. P.; and Pople, J. A. *GAUSSIAN 92/DFT,* Revision G.2; Gaussian Inc.: Pittsburgh PA, 1993.

(28) Hedberg, L.; Mills, I. M.; *J. Mol. Spectrosc.* **1993**, *160*, 117.

(29) Haase, J. *Z. Naturforsch., A* **1970**, *25A*, 936.

**Table 4.** Interatomic Distances and Vibrational Amplitudes from GED and from Scaled ab Initio (ai) Force Field[a]

| | dist | amplitude GED | amplitude ai |
|---|---|---|---|
| C═O | 1.17 | 0.037[b] | 0.036 |
| N═O | 1.19 | | 0.037 |
| C−F | 1.32 | 0.043 (3) | 0.043 |
| O−C | 1.36 | | 0.048 |
| O−O | 1.42 | | 0.045 |
| O−N | 1.51 | 0.054[b] | 0.054 |
| O4···O5 | 2.18 | 0.052[b] | 0.050 |
| O3···F | 2.23 | | 0.051 |
| O1···O3 | 2.28 | | 0.053 |
| O1···F | 2.11 | 0.063 (7) | 0.060 |
| O2···O4 | 2.21 | | 0.063 |
| C···O2 | 2.24 | | 0.064 |
| O2···O5 | 2.34 | | 0.059 |
| N···O | 2.34 | | 0.067 |
| O1···O5 | 2.52 | 0.102 (9) | 0.091 |
| O2···O3 | 2.56 | | 0.098 |
| C···N | 2.94 | 0.116[b] | 0.116 |
| C···O5 | 2.90 | 0.189 (23) | 0.170 |
| N···O3 | 3.03 | | 0.189 |
| O3···O5 | 3.09 | | 0.224 |
| O2···F | 3.37 | 0.076 (7) | 0.061 |
| O1···O4 | 3.40 | | 0.067 |
| O5···F | 3.79 | 0.254 (51) | 0.248 |
| O3···O4 | 3.87 | | 0.239 |
| C···O4 | 3.98 | 0.173 (27) | 0.129 |
| N···F | 4.04 | | 0.140 |
| O4···F | 5.18 | 0.133 (32) | 0.126 |

[a] Values in Å. Experimental uncertainties are $3\sigma$ values. For atom numbering see Figure 3. [b] Not refined.

to deviate from planarity. These deviations are described by the torsional angles $\tau$(FCO) and $\tau(NO_2)$. If both angles are positive, the O3···O5 distance decreases (see Figure 3 for atom numbering). Vibrational amplitudes were refined in groups according to their distances and according to the amplitudes obtained from the ab initio force field. Some amplitudes were constrained to the ab initio values (see Table 4). With these assumptions nine geometric parameters $p_i$ and eight vibrational amplitudes were refined simultaneously. Only two correlation coefficients had values larger than $|0.6|$: $p_6/p_8 = -0.72$ and $p_7/p_9 = -0.76$. The final results of the least-squares refinement are listed in Table 3 (geometric parameters) and Table 4 (vibrational amplitudes).

In the gas electron diffraction (GED) experiment, only the syn conformer of $FC(O)OONO_2$ is observed. This result is in agreement with the interpretation of the NMR spectra (see above) and with the matrix IR spectra which demonstrate the presence of a single conformer only, even at 200 °C. If we estimate from these spectra an upper limit of 5% of a second form, we obtain $\Delta G° = G°(\text{anti}) - G°(\text{syn}) > 2.8$ kcal mol$^{-1}$. $FC(O)OONO_2$ possesses a skew structure with a dihedral angle of $\phi(\text{COON}) = 86.2(14)°$. This is smaller than in most other peroxides which possess effective dihedral angles of 120° (120.0(5)° in $H_2O_2$[30]) or larger (123(4)° in $(CF_3)_2O_2$,[31] 135(5)° in $(CH_3)_2O_2$,[32] 144(6)° in $(SiMe_3)_2O_2$,[33] and 166(3)° in $t$-$Bu_2O_2$[33]). Gas phase structures with dihedral angles smaller than 90° were observed so far only for three compounds, $F_2O_2$[34] (88.1(4)°), $Cl_2O_2$[35] (81.03(1)°), and $(FC(O))_2O_2$[11] (83.5(14)°). The FC(O) and $NO_2$ groups in $FC(O)OONO_2$ are rotated by ∼5° from the orientations where the C═O3 and N═O5 bonds eclipse exactly the O−O bond. The direction of both rotations is such that the O3···O5 distance decreases. This distance (3.09 Å) is larger than the respective van der Waals distance (2.80 Å). The O−O bond in $FC(O)OONO_2$ (1.420(6) Å) is shorter than such bonds in $H_2O_2$[30] (1.475(4) Å) and $(CH_3)_2O_2$[32] (1.457(12) Å) but very similar to those in peroxides with electronegative substituents (1.419(9) Å in $(FC(O))_2O_2$,[11] 1.426(2) Å in $Cl_2O_2$,[35] or 1.419(20) Å in $(CF_3)_2O_2$[31]). A well known exception is $F_2O_2$ with O−O = 1.216(2) Å.[34] The N−O bond (1.514(6) Å) is much longer than that in $HONO_2$[36] (1.406(5) Å) and $CH_3ONO_2$[37] (1.402(5) Å) and is similar to such bonds in the halogen nitrates $ClONO_2$[26] (1.493(3) Å) and $FONO_2$[26] (1.507(4) Å). Since N−O bond lengths in $XO{-}NO_2$ compounds correlate with the electronegativity of X, the similar bond lengths in $FONO_2$ and $FC(O)OONO_2$ suggest that the electronegativity of the FC(O)O moiety is nearly equal to that of fluorine. This confirms the observation for the N═O stretching vibrations (see above). The long N−O bond reflects the chemical properties of $FC(O)OONO_2$, i.e., the easy rupture of this bond and thermal decomposition in FC(O)OO and $NO_2$ radicals.

The HF/3-21G and LDF/DZP methods reproduce the experimental geometry reasonably well, i.e., bond lengths better than ±0.03 Å and bond angles better than ±3°. A discrepancy between experiment and theory exists for the torsional angles of the FC(O) and $NO_2$ groups. The GED analysis results in similar values for both angles ($\tau(\text{FCO}) = 5.6(43)°$ and $\tau(NO_2) = 4.9(9)°$). The HF/3-21G method predicts a strong torsion of the $NO_2$ group ($\tau(NO_2) = 11.6°$) and a very small torsion of the FC(O) group ($\tau(\text{FCO}) = 1.2°$), whereas the LDF/DZP calculation predicts a minute torsion of the $NO_2$ group ($\tau(NO_2) = 0.1°$) and an intermediate torsion of the FCO group ($\tau(\text{FCO}) = 6.9°$). When the experimental and calculated dihedral angles $\phi$(COON) are compared, systematic differences must be taken into account. The vibrational average derived from the GED experiment may differ by several degrees from the equilibrium value. Considering this systematic difference, both theoretical methods reproduce the experimental diheral angle satisfactorily.

**Acknowledgment.** Finacial support by the Deutsche Forschungsgemeinschaft and Fonds der Chemischen Industrie is gratefully acknowledged.

IC960847P

---

(30) Redington, R. L.; Olson, W. B.; Cross, P. C.; *J. Chem. Phys.* **1962**, *36*, 1311.

(31) Marsden, C. J.; Bartell, L. S.; Diodati, F. P. *J. Mol. Struct.* **1977**, *39*, 253.

(32) Haas, B.; Oberhammer, H. *J. Am. Chem. Soc.* **1984**, *106*, 6146.

(33) Käss, D.; Oberhammer, H.; Brandes, D.; Blaschette, A. *J. Mol. Struct.* **1977**, *40*, 65.

(34) Hedberg, L.; Hedberg, K.; Ellen, P. G.; Ryan, R. R. *Inorg. Chem.* **1988**, *27*, 232.

(35) Birk. M.; Friedl, R. A.; Cohen, E. A.; Pickett, H. M.; Sander, S. P. *J. Chem. Phys.* **1989**, *91*, 6588.

(36) Cox, A. P.; Riveros, J. M. *J. Chem. Phys.* **1965**, *42*, 3105.

(37) Cox, A. P.; Waring, S. *Trans. Faraday, Soc.* **1971**, *67*, 3441.